A Machine-Learning Based Microwave Sensing Approach to Food Contaminant Detection

A Machine-Learning Based Microwave Sensing Approach to Food Contaminant Detection

Luca Urbinati, Marco Ricci, Giovanna Turvani, Jorge A. Tobon Vasquez, Francesca Vipiana, Mario R. Casu
Department of Electronics and Telecommunications
Politecnico di Torino, Torino, Italy 10129
Email: {mario.casu,francesca.vipiana}@polito.it

***Abstract*—To detect contaminants accidentally included in packaged foods, food industries use an array of systems ranging from metal detectors to X-ray imagers. Low density plastic or glass contaminants, however, are not easily detected with standard methods. If the dielectric contrast between the packaged food and these contaminants in the microwave spectrum is sensible, Microwave Sensing (MWS) can be used as a contactless detection method, which is particularly useful when the food is already packaged. In this paper we propose using MWS combined with Machine Learning (ML). In particular, we report on experiments we did with packaged cocoa-hazelnut spread and show the accuracy of our approach. We also present an FPGA acceleration that runs the ML processing in real-time so as to keep up with the throughput of a production line.**

I. Introduction

The quality of the production process is vital for the food industry. Consumer complaints, in an era where online reputation can make the difference between survival and death for a company, must be reduced as much as possible. Furthermore, for the food industry there is the problem of safeguarding consumer health. For these reasons, this industrial sector is constantly seeking for new and improved solutions to detect food contaminants that might accidentally be included in packaged foods.

The most common devices installed along a food production line are X-Ray imagers, metal detectors, and near-infrared (NIR) hyperspectral imagers. Terahertz imaging is also being adopted, but besides the high cost, it exhibits poor depth penetration, which limits its applicability. NIR imaging also suffers from low penetration depth. Ultrasound imaging requires contact between transducer and sample, which makes it not applicable to most packaged foods.

The devices currently in use cannot detect all potential contaminants. For example, low-density plastic or glass fragments, which can accidentally detach from the package during the packaging phase, are transparent for these devices. Although the occurrence of such events is rare, it is still of the utmost importance that these contaminants are detected.

Microwave Imaging (MWI) [1] is a technique that uses low-power electromagnetic waves in the microwave spectrum to reconstruct an image of the spatial distribution of the dielectric properties in an object. This is obtained by first radiating microwaves through a set of antennas and recording the scattered waves through the same antennas; then the recorded signals are processed with an algorithm that generates an image, which is further elaborated to locate targets or to distinguish different materials. This is possible because two different materials in contact create a discontinuity that scatters an incident wave more or less depending on the difference between the dielectric properties of the two materials.

Although MWI can be used to detect contaminants in packaged foods, we take a slightly different route. We still use microwaves to illuminate the object and record the scattered waves, but instead of running a computationally expensive imaging algorithm, which might not be appropriate for real-time detection in a food production line, we train a Machine-Learning (ML) classifier to work directly on the raw microwave signals. We refer to this approach as ML-based Microwave Sensing (MLMWS).

To the best of our knowledge, we are the first to use this approach for contaminant detection in packaged foods, although the combination of microwave sensing and machine learning is not new and has been applied to the biomedical field first [2][3]. In particular, we use MLMWS to detect plastic and glass contaminants in cocoa-hazelnuts spread packaged in glass jars with a plastic cap. We use an array of six antennas working at 10 GHz connected to a switching matrix, which in turn is connected to a Vector-Network Analyzer (VNA). This system generates a 6×6 S-matrix of scattering parameters for each measurement. We collected several of these scattering matrices related to jars with and without contaminants and created a dataset of labeled data. Then we trained two ML classifiers, a Support Vector Machine (SVM) and a Multilayer Perceptron (MLP), to determine which one worked best for this application. Finally we implemented the best found MLP in hardware on an FPGA to guarantee a real-time execution.

In this paper we report on our work on MLMWS. More in detail, Sec. II makes a brief summary of the state of the art. Sec. III describes the Microwave Sensing (MWS) system that we use in our experiments. Sec. IV describes the ML training and reports the experimental results and the design of the ML hardware accelerator. Finally, Sec. V concludes the paper.

II. Related Work

Following the successful application of MWI to the medical imaging field [4], there has been an increasing interest toward industrial applications of this technique [5]. There is not abundant literature about MWI and MWS applied to the food industry. The only noteworthy exceptions [6]-[8] focus on

978-1-7281-3320-1/20/$31.00 ©2020 IEEE

sensing rather than imaging, which is also the focus of our contribution in this work.

The authors of [6] developed a hand-held time-domain reflectometer working in the microwave spectrum to assess the food quality by measuring variations in the dielectric properties, which can be determined by a variation of water concentration. Our goal is different, since we focus on detecting foreign bodies in packaged food, and since our system needs to be installed in an automated production line.

Using radar-based MWS for food screening—and so potentially also for detecting foreign bodies—has been suggested in [7], but without experiments to prove feasibility and accuracy. An industrial implementation of radar-based detection of foreign contaminants, however, is currently commercialized [8]. The radar can detect foreign bodies such as wood, plastic, bone, and fruit stones but is fundamentally different from our approach as it applies to pipes where liquid food or emulsions can flow before being packaged.

III. Microwave Sensing System

The MWS radiating system consists of six PCB-printed monopole antennas arranged in an arch lying above the production line and under which the jars flow uninterrupted. The antennas resonate around 10 GHz. This frequency, which we selected after extensive numerical simulations, represents a good trade-off between penetration depth (the lower the better) and resolution (the higher the better) [9]. The volume covered by the field radiated by the antennas is a cylinder with section $\sim$200 cm^2 and height $\sim$13 cm. The jars that we use in our experiments have a section of diameter 6.6 cm and height 7.5 cm, but changes in size are possible as long as the jars fit under the arch.

The antennas are connected to a 2×6 custom-made, electro-mechanical switching matrix, which in turn is connected to a 2-port VNA. A picture showing the entire MWS system is in Fig. 1. To collect the experimental data, we use a laptop connected to the VNA. In a fully engineered industrial system, the laptop will be replaced by a compact embedded system.

By properly configuring the switching matrix, it is possible to activate any transmitting path from one VNA port to one transmitting antenna, and any receiving path from one receiving antenna to the other VNA port. Thus, we can measure a 6×6 scattering matrix by activating all the possible antenna pairs, including the monostatic combinations in which the same antenna is used as both transmitter and receiver. Due to reciprocity, the S-matrix is symmetrical. In our approach we do not use the monostatic cases that correspond to the diagonal elements of the matrix. As a result, due to symmetry and the fact that the diagonal elements are not needed, only the fifteen elements of the upper triangular part of the S-matrix are actually measured, which shortens the acquisition time.

To automate the measurements, a photocell triggers the VNA and the switching matrix every time a new jar is about to pass under the arch. We performed our experiments on an industrial production line with an operating speed of around 30 cm/s and an average distance between jars of around 10 cm. This sets a constraint of around 333 ms to perform one measurement and to process the data. The fifteen measurements require in total a few tens of milliseconds, due primarily to the electro-mechanical swithing time, whereas the VNA measurement time is less than one millisecond. This means that the measurements are like a sequence of snapshots of a moving subject (i.e. the jar) that spans around 1.5 cm between the first and last snapshot. In MWI this might have a significant impact on the image resolution. For our ML-based sensing approach, the movement of the target is much less relevant, especially considering that it is taken into account in the development of an adequate training set.

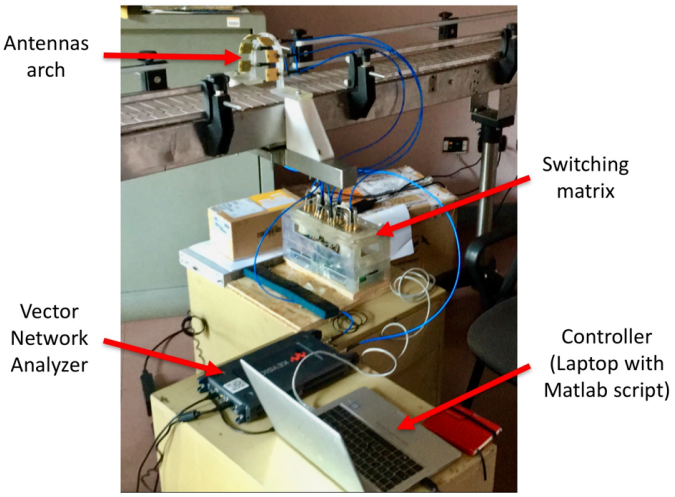

Fig. 1: Picture showing the MWS system.

IV. Machine Learning

The diagram in Fig. 2 describes the design flow to obtain the final implementation of the selected ML algorithm on an FPGA starting from the collection of the Dataset. Subsection IV.A and IV.B report on the first two blocks and the last three blocks of the diagram, respectively.

A. ML design

First of all, the MWS system is used to create a balanced Dataset obtained by measuring 1200 contaminated and 1200 uncontaminated samples (first block in Fig. 2). For practical reasons, each sample is a jar filled with safflower oil instead of hazelnut-cocoa spread. The motivation is that the two liquids have the same dielectric constant ($\sim$2.86 at 10 GHz), which makes them behave in the same way in the microwave spectrum, but the oil is optically transparent, which facilitates the positioning and monitoring of the contaminants in the experiments. These foreign bodies are (in brackets the max./min. dimensions or the diameter): a metal sphere (10 mm), a glass fragment (13/2 mm), a big plastic sphere (20 mm), a small plastic sphere (3 mm), a triangular plastic fragment (8/1 mm), and a cap shape plastic (15/9 mm).

For each type of foreign body, 200 samples are measured, changing their position in the jar: in the middle, at the surface,

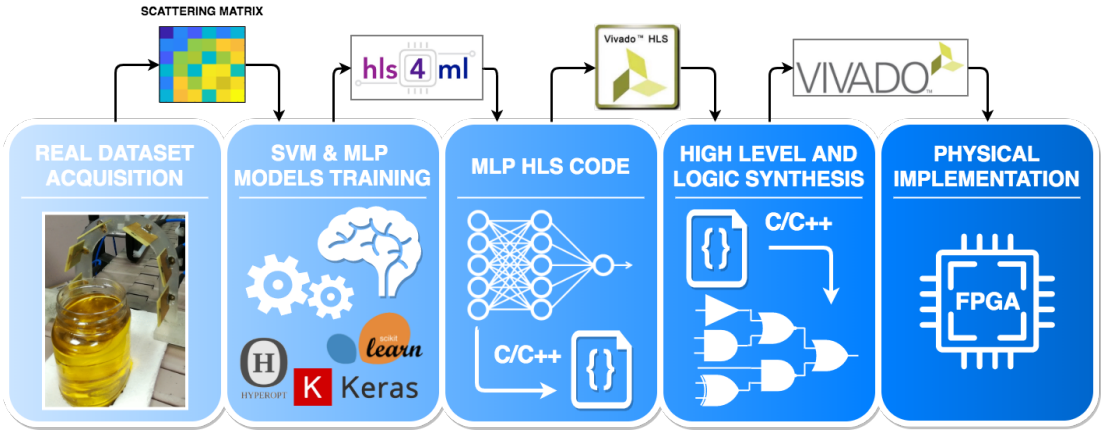

Fig. 2: Flow diagram representing the activities carried out in this work.

and in the horizontal plane at fixed height. The diversity of the Dataset is further increased by rotating the sample in a range of $\pm 10^{\circ}$ with respect to its long-side axis and by displacing it by $\pm$2cm from its ideal position under the antennas arch.

For each sample, the fifteen elements of the triangular upper part of the 6×6 S-matrix are recorded. Since each of these elements is a complex number with real and imaginary parts, each sample in the Dataset is a vector of $15 \times 2 = 30$ features.

The second block in Fig. 2 uses the Dataset to determine the best ML algorithm for the classification of the samples. As a preliminary step, the Dataset is shuffled and split in a *Training Set* made of 80% of the data and a *Test Set* composed by the remaining 20%. To keep these subsets balanced, their number of "contaminated" and "free" samples are the same. Next, standardization with *StandardScaler* [10] is applied first to the Training Set, then to the Test Set.

With the standardized Training Set, two binary classifiers are trained: a Support Vector Machine (SVM) [15] and a Multilayer Perceptron (MLP) [11]. The SVM is chosen because it is easy and fast to train, since it has only two hyper-parameters if the Radial Basis Function (RBF) kernel is used (the regularization parameter C and the kernel-specific parameter γ), and because it can be used to judge on the suitability of ML altogether to solve the problem at stake [11]. In addition, SVM has been applied effectively to other detection problems using microwaves, like breast-cancer monitoring [12]-[14]. MLP is chosen as the second classifier because, although slightly more difficult than SVM to train, it is more suitable for a real-time hardware implementation, which could favor this choice in case the discriminating capacity is satisfactory.

The key points of the SVM training procedure are [16]:

1) consider the Radial Basis Function (RBF) kernel;
2) adopt a loose grid with 5-fold cross-validation (CV) and a fine grid with 10-fold CV;
3) use CV and *Grid-Search* to find the best hyper-parameters (C, γ) that maximize the CV accuracy;
4) train the SVM on the entire Training Set with best (C, γ).

Regarding MLPs, we designed three architectures, each with 30 Units in the Input Layer (as many as the number of features) and only one Sigmoid Unit in the Output Layer to let the MLP work as a binary classifier. The three MLPs differ in the number of *hidden layers:* 1, 2 or 3. More than three hidden layers would not probably bring about any advantage [18].

Training these MLPs with Grid-Search would be too time-consuming because of the many hyper-parameters to tune. Therefore, we used Bayesian Optimization (BO), also known as Sequential model-based optimization (SMBO), thanks to the Hyperopt Library [17]. The training procedure is as follows:

1) define constant non-tunable hyper-parameters: Adam Optimizer, Binary Cross-Entropy Loss Function, L2 Weight Regularization (active when Regularization Parameter is greater than 0), 1000 as maximum number of Epochs;
2) define loose and fine grids for each tunable hyper-parameter: number of Units per Hidden Layer as powers of 2; Relu, Selu, and Tanh as Activation Functions; He Normal, Lecun Normal, and Glorot Normal as Weight Initializers; Weight Regularization Parameter from 0.0 to 0.1 in logarithmic scale; Dropout Rate from 0.0 to 0.55; 10, 50, and 100 as Batch-size;
3) carry out 5-fold CV and BO to select the most promising hyper-parameters that minimize the validation loss. Use early-stopping to monitor the validation loss, with 10 epochs of patience and a triggering condition of 0.002;
4) train new MLPs from scratch with the promising hyper-parameters on 75% of the Training Set, using the 25% as Validation Set (arbitrary choice). At the epoch that provides the lowest validation loss, weights and architectures of the model are saved for a possible subsequent hardware implementation. The saving procedure is not done directly during the 5-fold CV training phase because it would have slowed it down.

To perform the ML experiments with the two kinds of classifiers, we used various Python libraries, of which the main ones are: *scikit-learn* 0.21.3, *keras* 2.2.4, and *hyperopt* 0.1.2.

As a final step, to evaluate and compare the generalization performance of the SVMs and the MLPs, the most promising models (those with the highest validation accuracy) have been tested on the held-out 20% of the Dataset.

The best SVM has (C, γ) = (56.0, 0.027), Test Accuracy 93.958%, and Error Rate 6.042% as it mispredicts 29 samples out of 480 of the Test Set (22 False Negatives and 7 False Positives). Its Area Under the ROC Curve (AUC) is 0.982.

The winning MLP has 2 Hidden Layers with [128, 256] Relu Units. It also mispredicts 29 out of 480 samples, which leads to the same Error Rate of 6.042%, even though the balance of False Negatives and Positives is slightly different (21 False Negatives and 8 False Positives). Its AUC is 0.980.

Tab. I reports the errors of both classifiers on the Test Set. The reason why the triangular plastic fragment determines the largest number of errors is not its small dimensions, but rather the fact that it always floats on the surface of the liquid in the jar. As a result, the low dielectric contrast of the plastic-oil interface with respect to the plastic-air one makes the fragment almost invisible in the back-scattered signal. This is clearly an aspect that needs further investigation in future works.

Type of Sample	**Occurrences in Test Set**	**SVM Errors → Error Rate (%)**	**MLP Errors → Error Rate (%)**
Free = No contaminant	240	7 → 2.917	8 → 3.333
Metal sphere	45	1 → 2.222	0 → 0
Glass fragment	43	1 → 2.326	0 → 0
Big plastic sphere	37	0 → 0	0 → 0
Small plastic sphere	35	0 → 0	0 → 0
Triang. plastic fragment	41	20 → 48.780	21 → 51.220
Cap shape plastic	39	0 → 0	0 → 0
Sum	480	29 → 6.042	29 → 6.042
Sum without triang. plastic fragment	439	9 → 2.050	8 → 1.822

TABLE I: Types of samples in the Test Set and their contribution to the final Error Rate for both SVM and MLP.

Based on these results, we chose the MLP classifer for hardware implementation over the SVM one because:

- it has lower False Negatives, which are more important than False Positives because jars with foreign bodies must be eliminated at all costs, including wasting some jars declared as contaminated even if they are free;
- it correctly predicts all the hazards, except the triangular plastic fragment, which is also the defect of the SVM;
- its hardware realization is simpler and faster;
- it has the same Error Rate of the SVM on the Test Set.

B. Hardware Acceleration

To implement on FPGA the Hardware Accelerator for the best found MLP, the first step is to produce a synthesizable code, which corresponds to the transition between the second and the third block in Fig. 2. For this, we used the *hls4ml* tool [19], which converts the MLP Keras model (architecture and weights) in a C/C++ code. This code is ready to be synthesized in hardware using the High-Level Synthesis (HLS) design flow of Vivado HLS, which is the Xilinx FPGA development tool. In fact, our target FPGA is the Xilinx xc7z020clg484-1 mounted on the ZedBoard Zynq-7000 Development Board.

The HLS code produced by *hls4ml* needs to be edited to add the Standardization Block, which standardizes the inputs with the mean and standard deviation values obtained during a preprocessing phase[1]. In this way, new unseen samples undergo the same standardization of the training samples: this is a crucial step to make the MLP work as expected.

In the conversion from Keras to HLS, *hls4ml* allows configuring clock period, internal fixed-point precision, pipelining, resource reuse, etc. Different combinations of those settings are tested, with the goal of maintaining the correct functionality, the latency under 100 ms, and the resource utilization below the limits of the target FPGA.

To select the best implementation, many simulations in Vivado HLS with various configurations have been performed. This activity corresponds to the fourth block in Fig. 2. The results matched the predictions of the Keras MLP only for the cases with precision no less than <64, 32>, where 64 is the internal bit-width parallelism and 32 (out of 64) are the fractional bits. Therefore, we selected this precision in our final implementation. For reasons of space we cannot provide more details about the other configuration parameters that we set to minimize the computation latency.

After the physical implementation, which is the last block in Fig. 2, we obtain the results in Tab. II in terms of performance, utilization of FPGA resources, and power.

Freq. (MHz)	**Latency (ms)**	**BRAMs (%)**	**DSPs (%)**	**FFs (%)**	**LUTs (%)**	**Power (W)**
100	2.997	43	11	9	14	1.974

TABLE II: Characteristics of the solution implemented on FPGA.

V. Conclusion

In this paper we have shown how the combination of Microwave Sensing and Machine Learning can detect the presence of contaminants in packaged jars when the liquid has different dielectric properties than the foreign bodies. Our thorough ML design procedure led to select the best Support-Vector Machine and Multi-Layer Perceptron classifiers, of which the last was implemented in FPGA to guarantee real-time performance in the industrial environment. The focus of future investigation will be on improving the accuracy for some particular contaminants.

Acknowledgment

This work was supported by the Italian Ministry of University and Research under the PRIN project BEST-Food – Broadband Electromagnetic Sensing Technologies for Food Quality and Security Assessment. We also thank Nutkao Srl for providing the test samples and the design requirements.

[1]The preprocessing phase aims to normalize the input features so that none of them influence the training phase more than the others [18].

REFERENCES

[1] Pastorino M., Microwave Imaging, Whiley, 2010.

[2] Persson M. *et al.,* "Microwave-Based Stroke Diagnosis Making Global Prehospital Thrombolytic Treatment Possible," *IEEE Transactions on Biomedical Engineering,* vol. 61, no. 11, pp. 2806-2817, Nov. 2014.

[3] Bahramiabarghouei H., Porter E., Santorelli A., Gosselin B., Popović M., Rusch L. A. , "Flexible 16 Antenna Array for Microwave Breast Cancer Detection," *IEEE Transactions on Biomedical Engineering,* vol. 62, no. 10, pp. 2516-2525, Oct. 2015.

[4] Chandra R., Zhou H., Balasingham I., Narayanan R. M. , "On the Opportunities and Challenges in Microwave Medical Sensing and Imaging," *IEEE Transactions on Biomedical Engineering,* vol. 62, no. 7, pp. 1667-1682, July 2015.

[5] Wu Z., Wang H., "Microwave Tomography for Industrial Process Imaging: Example Applications and Experimental Results," *IEEE Antennas and Propagation Magazine,* pp. 61–71, Volume: 59 Issue: 5, 2017.

[6] Schimmer O., Daschner F., Knochel R., "UWB-Sensors in Food Quality Management—the Way From the Concept to Market," in *2008 IEEE International Conference on Ultra-Wideband,* Hannover, 2008, pp. 141-144.

[7] Edwards M., "Detecting Foreign Bodies in Food," Woodhead Publishing Ltd, 2004.

[8] Food Radar. Accessed: 01/23/2020. http://www.foodradar.com/

[9] Tobon V. J., Rivero J., Scapaticci R., Farina L., Crocco L., Vipiana F., "Monitoring of Food Contamination via Microwave Imaging," in *2019 International Applied Computational Electromagnetics Society Symposium (ACES)*, pp. 1-2, 2019.

[10] scikit-learn developers (2019). scikit-learn user guide. *Release 0.21.3*. Accessed: 01/23/2020. https://scikit-learn.org/stable/_downloads/scikit-learn-docs.pdf

[11] Nielsen M.A., Neural Networks and Deep Learning, Determination Press, 2015. Accessed: 11/14/2019. http://neuralnetworksanddeeplearning.com/index.html

[12] Conceicao R. C., Hugo Medeiros M., O'Halloran, Rodriguez-Herrera D., Flores-Tapia D., Pistorius S., "SVM-based Classification of Breast Tumour Phantoms Using a UWB Radar Prototype System," in *2014 XXXIth URSI General Assembly and Scientific Symposium (URSI GASS)*, pp. 1-4, 2014.

[13] Byrne D., O'Halloran M., Jones E., Glavin M.. "Support Vector Machine-Based Ultrawideband Breast Cancer Detection System," *Journal of Electromagnetic Waves and Applications,* 25.13, pp. 1807-816, 2011.

[14] Sacristán J., Oliveira B. L., Pistorius S., "Classification of Electromagnetic Signals Obtained from Microwave Scattering over Healthy and Tumorous Breast Models," in *IEEE Canadian Conference on Electrical and Computer Engineering (CCECE),* pp. 1-5., 2016

[15] Cortes C., Vapnik V., "Support-Vector Networks," *Machine Learning,* Vol. 20, No. 3, pp. 273-297, Sep. 1995.

[16] Hsu CW., Chang CC., Lin CJ, A Practical Guide to Support Vector Classification. *National Taiwan University, Taipei 106, Taiwan*. Accessed: 11/13/2019. https://www.csie.ntu.edu.tw/~cjlin/papers/guide/guide.pdf

[17] Bergstra J., Yamins D., Cox D.D. "Hyperopt: A Python Library for Optimizing the Hyperparameters of Machine Learning Algorithms," in *Proceedings of the 12th Python in Science Conference (SciPy 2013).*, pp. 1-8.

[18] Duda R., Peter E., Stork. D. G., Pattern classification. *Wiley, New York, 2nd Edition.*, 2001.

[19] Duarte J. *et al.,* "Fast Inference of Deep Neural Networks in FPGAs for Particle Physics." *Journal of Instrumentation,* Vol. 13, July 2018.